Wind turbine wake stability investigations using a vortex ring modelling approach

Daniel Baldacchino and Gerard J. W. van Bussel
Delft University Wind Energy Research Institute, Faculty of Aerospace Engineering, Kluyverweg 1, 2629 HS Delft, The Netherlands.
E-mail: d.baldacchino@tudelft.nl

Abstract. In the present study, a simple inviscid vortex ring (VR) modelling approach is used to represent the developing rotor wake. This allows a straightforward investigation and comparison of the impact of uniform, yawed and sheared flow conditions on the development of the rotor wake, with the additional possibility of including ground effect. The effect of instabilities on the development of the wake is manually introduced in the form of perturbations of strength, ring position and size. The phenomenon of vortex filament interaction or *leapfrogging*, could play a role in the observation of unsteady phenomena and is therefore also addressed. Such a study is hence performed in light of recent conflicting views on the causes of wake meandering: is the observed dynamic wake behaviour a result of large scale turbulent forcing or do more subtle and intrinsic wake instabilities play a role?

This study concludes that the presence of the ground and external perturbations, most notably changes in the wake pitch and the rotor thrust coefficient, can significantly affect the steady development of the wake. The mutual vortex pairing instability, whilst displaying interesting periodic behaviour, does not correlate with periodic wake behaviour reported by Medici et al. [1]. However, in the absence of unsteady inflow, it is shown that the wake of a Horizontal Axis Wind Turbine (HAWT) is certainly prone to displaying unstable, dynamic behaviour caused by these additional factors.

1. Introduction

Wind turbine wakes are characterised by velocity deficits and increased turbulence levels, affecting turbine loads as well as power production levels in wind farms. In addition, recent wind tunnel and field observations (see e.g. [1, 2, 3]), revealed that wakes do not propagate steadily behind the rotor, but rather have a tendency to oscillate randomly, a phenomenon dubbed "wake meandering". This has important implications for turbines operating within wakes of other turbines.

Recent work by Larsen et al. [4] investigated this wake meandering phenomenon based on the hypothesis that the wake behaves as a passive tracer, governed by large-scale lateral and horizontal turbulent components. In contrast, Medici and Alfredsson [1] propose that a meandering mechanism similar to bluff body vortex shedding is responsible for an oscillatory signal detected in the wake of a two-bladed turbine model. Specifically, a low frequency velocity signal was detected by said authors in the near wake of the model rotor immersed in a boundary layer wind tunnel. They additionally investigated different types of actuator disks and turbine models to ascertain the influence of disk porosity and turbine solidity on the observed frequency spectra. The authors state that their experimental data is supported by low frequency peaks reported in field wake measurements in the Alsvik wind farm [5].

A follow up study was conducted by Sørensen and Okulov [6] using an analytical helical wake model and a similar velocity signal as found in [1] was obtained. The underlying meandering mechanism is however not fully addressed since the vortex wake model was specifically tuned to obtain a matching velocity signal.

Despite doubts over the choice of experimental parameters in [1], the overall outcome highlights the uncertainty in our current understanding of the meandering phenomenon. This is what motivated the present research question: what is the root cause for the observed wake meandering phenomenon?

Additional studies pertaining to the stability of the wake have addressed the inherent structure of the wake, and conditions for wake stability. Most notably are analytical and experimental studies by Widnall et al. [7], as well as in Sørensen and Okulov [8]. More recently Stack et al. [9] reported observing the so-called *Widnall instabilities* in controlled investigations in the wake of a hovering rotor. Similarly, Felli et al. [10] produced numerous detailed snapshots of an evolving propeller wake and observed all three of the documented *Widnall instabilities*, one of which is the mutual pairing instability, or leapfrogging mode, observed when adjacent vortex filaments with similar strength come into close contact.

2. Approach overview

To offer insight into the stability of the wake, an analytical modelling approach is taken to avoid truncation errors introduced by traditional computational methods. A simple Free-Wake Vortex Ring Model (FWVRM) is developed where the wind turbine rotor is assumed to have a constant load distribution, resulting in the sole generation of tip vortices. No root vortex is modelled, which also implies that the rotation of the wake is excluded from the analysis. For high tip speed ratios, these helical tip vortices have a small pitch (closely spaced). This enables the use of vortex ring elements to represent the helical rotor wake. The model allows for the inclusion of external factors such as ground effect. Furthermore, non-uniform inflow such as wind shear and yaw can be incorporated.

The availability of an analytical solution for the induced velocities of infinitely thin, inviscid, axisymmetric vortex rings (ideal vortex rings) means they are particularly well suited to represent the wake in the desired simplistic manner. In the modelling approach, the vortex rings are treated as rigidly expanding bodies so as to incorporate wake expansion as well as to allow for the inclusion of out-of-plane vortex-ring rotations. The latter are of prime importance for capturing wake tilting and skewing due to velocity imbalances around the ring peripheries. The derived quasi-3D model, building on previous work of Øye [11] and Micallef et al. [12], is able to simulate these effects enabling the calculation of the induced velocity at any point in space.

The free-wake model works by initiating a new vortex ring every rotor blade passage, thus representing the helical tip vortices from each blade, collapsed onto a single ring. The influence of each ring on one another is evaluated by averaging the velocity components acting on each ring periphery. Any resulting imbalances lead to lateral displacements, skewing and/or tilting of the rings. The resulting ring orientations are then approximated kinematically by treating the rings as solid bodies. Wake expansion is modelled using an exact expression for the velocity along the centreline of a cylindrical sheet of vorticity as given in Wilson [13] and using the principle of mass conservation.

Furthermore, the effect of the ground is modelled using the ground mirroring technique. Artificial perturbations can be introduced by distorting the vortex rings. Examples are distortions in the position, strength or the local radii of the rings, representing low frequency turbulence.

Generalisation of the model also allows for an investigation of the interaction of co-rotating,

Journal of Physics: Conference Series **555** (2014) 012111 doi:10.1088/1742-6596/555/1/012111

co-axial vortex rings, whereby the mutual and self-induced axial and radial velocities at each ring are easily evaluated, providing insight into the nature of vortex filament interaction and its relevance to wind turbine wakes.

3. Model description

3.1. Analytical vortex ring expressions

The exact solution for the induced axial and radial velocities (u_z, u_r) at a point (z, r), from a thin vortex ring of strength Γ_i and radius R_i, with its centroid at$(z_i, 0)$, are given by:

$$u_z = \frac{\Gamma_i}{2\pi\sqrt{[(z-z_i)^2+(r+R_i)^2]}} \cdot \left[K(m) + \frac{R_i^2 - r^2 - (z-z_i)^2}{(z-z_i)^2+(R_i-r)^2}E(m)\right] \quad (1)$$

$$u_r = \frac{\Gamma_i(z-z_i)}{2\pi r\sqrt{[(z-z_i)^2+(r+R_i)^2]}} \cdot \left[K(m) - \frac{R_i^2 + r^2 + (z-z_i)^2}{(z-z_i)^2+(R_i-r)^2}E(m)\right] \quad (2)$$

where $K(m)$ and $E(m)$ are elliptic type integrals of the first and second kind, expressed in terms of the parameter $m = 4rR_i\left[(z-z_i)^2+(r+R_i)^2\right]^{-1}$. Evaluation of these integrals has been treated rigorously in literature; the method of Abramowitz and Stegun [14] is adopted here. The same notation as used in [12] and [15] is maintained for consistency.

The self-induced velocity component of an ideal vortex ring is described in its simplest form, which is obtained by evaluating the axial velocity component (equation 1) at the ring centroid. The velocities calculated in this manner are described in terms of the local vortex ring coordinate system. Thus we have the simple expression:

$$u_z(z = z_i, r = 0) = \frac{\Gamma_i}{2R_i} \quad (3)$$

Expressing the self-induced velocity in this simple form bypasses ambiguities in explicitly defining a viscous core model, as is required with more common expressions, such as Kelvin's formula [16]. For very small core radii ($r_c/R < 0.01$), the aforementioned methods yield almost identical results.

In order to correctly capture the full dynamics of the wake, it is required to describe the induced velocities from arbitrarily oriented vortex rings. The equivalent point method as described in [12] is similarly followed in the current approach and implemented to further account for ring skewing due to shear and ground effects, as well as tilting due to yawed inflow (rotation about the x and y axes respectively).

3.2. Accounting for tilting and skewing effects

The vortex ring elements representing the wake give rise to mutually induced velocities within the wake. To evaluate the motion of the wake due to these mutual effects, velocities are evaluated at points on the perimeter of the rings. A weighted velocity average is found and subsequently used to estimate the turning effect on the ring about the x and y axes.

The ideal vortex rings which represent the wake are deformable only in the radial direction, i.e. flow conservation and the radial induced velocity field lead to changes in the ring radii. This means that the wake evolution description is limited here to the translation, rotation and expansion/contraction of the vortex rings.

3.3. Ground effect modelling

The proximity of the vortex wake to the ground may give rise to subtle yet notable effects. This phenomenon has long been treated from the perspective of aircraft aerodynamics, where aircraft within a wingspan of the ground experience an increase in lift. Wind tunnel experiments most commonly simulate this by employing the mirror image method. In numerical simulations, a similar approach can be taken. For simulating in-ground effect (IGE) aerodynamics, the reflection model is theoretically implemented by superposing an additional mirrored wake in the domain as shown in Figure 1a. In this case, a wake vortex ring is reflected about the $x - z$ plane (the ground plane) and its sense of strength is also reversed, enforcing an impermeable condition at the ground plane as illustrated in Figure 1b.

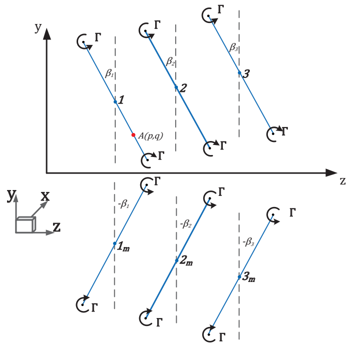

(a) Vortex ring system in ground effect

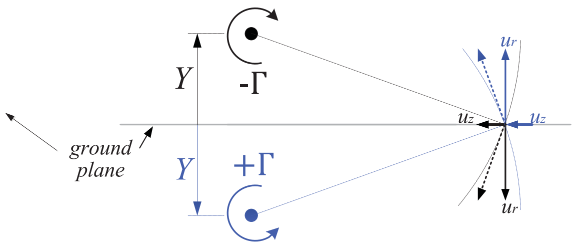

(b) Ground mirroring principle

Figure 1: Principles of the mirror imaging method

For a more detailed illustration of the effect on the induced velocity field arising from ground proximity, the reader is referred to Appendix A for velocity contours and vector plots for a sample dual-ring system IGE with a similar sense of strength as shown in Figure 1a.

3.4. Model parameters and relevance to HAWT wake modelling

For the wake evolution simulations, a single turn of B helical sheets of the wake originating from B blades are collapsed onto a single vortex ring, modelling therefore only the rolled-up situation of the helical wake, by a single tip vortex ring. This implies an actuator disk with a uniform loading as no intermediate or root vortex rings are modelled. This means that no wake rotation is accounted for in the simulations. Constraining the rotation of the wake, as well as the solid-body modelling of the vortex rings means that short- and long-wave instabilities cannot be predicted by the presented simplified model. The latter modes of instability were also identified by Widnall [7], together with the mutual pairing instability, which is the subject of this paper.

3.4.1. Free wake simulations It is of interest to identify the effect of perturbations on the development of the wake using the simple model developed. The procedure initiates with a tip ring being shed after a time step ΔT, set for instance according to a typical tip speed ratio $\lambda = 5$ for an $R = 50m$ rotor, at a wind speed of $10m/s$. The first ring is shed at a spatial location behind the rotor based on the total velocity at the rotor plane at $t = 0$. The orientation is similarly estimated through the average-moment method described in Section 3.2, estimating the tilting and skewing effects at the rotor plane. Subsequently, within the wake, each ring's position is updated by evaluating the velocities and moments on the periphery of the ring and using a first-order forward Euler scheme to estimate the new ring position and orientation.

The expansion of the wake is estimated using axial cylinder theory due to Wilson [13]. Depending on the ring's position downstream of the rotor, as well as the instantaneous axial induced velocity at the rotor plane, the radius of the ring is estimated based on this mass conservation expression.

An approximate expression for the strength of the shed vortex rings can be obtained from simple vortex theory of a uniformly loaded actuator disk, generalised for off-design operation:

$$B\Gamma = (B\Gamma_{opt}) \cdot \frac{3}{2} \cdot \left(1 - \frac{1}{3} \cdot \frac{\lambda}{\lambda_{opt}}\right) \tag{4}$$

where

$$(B\Gamma_{opt}) = \frac{\pi \cdot U_\infty \cdot C_{T(opt)} \cdot R}{\lambda_{opt}} \tag{5}$$

where B is the number of rotor blades, U_∞ is the freestream velocity and $C_{T(opt)}$ and λ_{opt} are the optimum thrust coefficient and tip speed ratio. The quantity $(B\Gamma)$ represents the total bound vorticity on the rotor, subsequently assigned as the ring strength.

3.4.2. Interacting vortex rings For the interaction study of a system of vortex rings, the analytical equations 1-2 are coupled with the self-induced velocity expression and solved using a simple forward Euler scheme with a minimum time step of $\Delta t = 0.0001s$ to ensure convergence. It is understood that in practice, even in the most ideal of conditions, the mutual interaction of vortex rings is seldom observed at length due to the rapid onset of vortex breakdown after the pairing event. However, for these inviscid simulations, two vortex rings which initiate leapfrogging should remain doing so indefinitely. It is also known that one such condition for initiating and maintaining the leapfrogging instability is that two rings are initially perfectly aligned coaxially. Any departure from this ideal can result in some initial interaction, soon to be followed by ring merging and breakdown.

Various trajectory investigations were carried out to observe the behaviour and limitations of vortex ring mutual interactions using the present model. Validating such results is vital but not straightforward due to lack of detailed data in literature. Unique results are found in Meleshko [17], who treated the subject of vortex ring interaction extensively and presents results of the modified *Dyson Model* for the case of two and three vortex ring systems. Said author [17] claims that the presented trajectories have been partially validated experimentally. These results are hence considered here as a means of validation for the present model.

4. Results and discussion

4.1. Wake development scenarios

Simulations are performed for freely-convecting rings to study the effects of instabilities on the evolution of the wake.

Lateral wake deflection is observed in the case of yawed inflow. Sample wake centreline trajectories are shown in Figure 2a. An increasing yaw angle causes a corresponding offset in the wake centreline, in the direction of the yawed wind direction. Interestingly, the model also predicts a degree of skewing in the wake, shown qualitatively in Figure 2d. The skew angle has been estimated between the rotor plane and a location $1D$ downstream. The wake induced velocity on the local flow conditions causes the wake structure to veer towards the downwind side. This phenomenon has been widely observed in numerous wind tunnel experiments and numerical simulations.

The influence of sheared inflow is examined by defining a simple power-law wind speed distribution $U(y)$ with the height above ground level, hh,

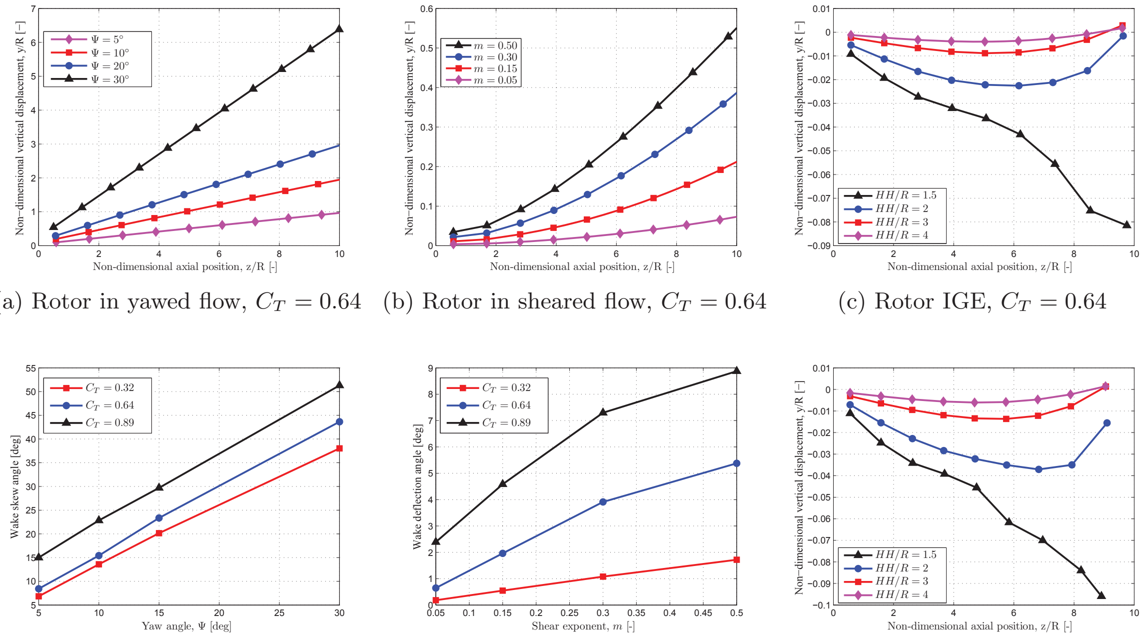

(a) Rotor in yawed flow, $C_T = 0.64$ (b) Rotor in sheared flow, $C_T = 0.64$ (c) Rotor IGE, $C_T = 0.64$

(d) Wake skew angle in yaw (e) Wake deflection due to shear flow (f) Rotor IGE, $C_T = 0.89$

Figure 2: Wake centreline properties for a yawed and sheared inflow, and for a rotor IGE.

$$U(y) = U_{hh} \cdot \left(\frac{y}{y_{hh}} \right)^m \tag{6}$$

where the axial wind velocity $U(y)$ at an arbitrary height y is defined in terms of the hub height wind velocity U_{hh} and the shear exponent m. The higher wind speed in the upper section of the rotor gives rise to a downward rotation of the wake structure, in this case rotating the wake vortex rings in the -β direction. Local effects due to the self-induced velocity however cause an overall upward shift of the wake structure. This is illustrated in Figure 2b, where the impact of stronger shear is also shown to cause a larger wake deflection. A higher operating thrust coefficient also tends to increase the deflection of the wake as shown in Figure 2e. These trends have been reported in a number of recent numerical studies (e.g. [12] and [18]).

The proximity of the rotor wake and the ground effectively accelerates the flow in a decreasing manner, upon moving upward and away from the ground plane (seen in Figure A1c). This would cause an upward rotation of the wake structure and the wake would tend to "lean" forward in the positive tilt direction (+β direction in Figure 1a). However, local vertical components of the vortex ring self-induced velocity come into play as the rings tilt. Hence the resultant effect is for the wake to tilt positively and shift downwards towards the ground. This downward shift in the wake structure has been observed experimentally ([19],[20]) as well as in numerical simulations ([21]) and is being attributed here to the self-induction of the wake itself. In this manner of description, the mechanism by which the wake structure shifts downward when in ground effect is similar to the up-shifting behaviour observed in shear flow.

As expected, the down-shift imparted onto the wake gradually increases as the relative hub height decreases (Figure 2c). The down-shift is also more prominent for higher values of the thrust coefficient (Figure 2f). Thrust values above the optimum resulted in chaotic centreline trajectories as substantial vortex ring interaction led to unrealistic vortex ring behaviour.

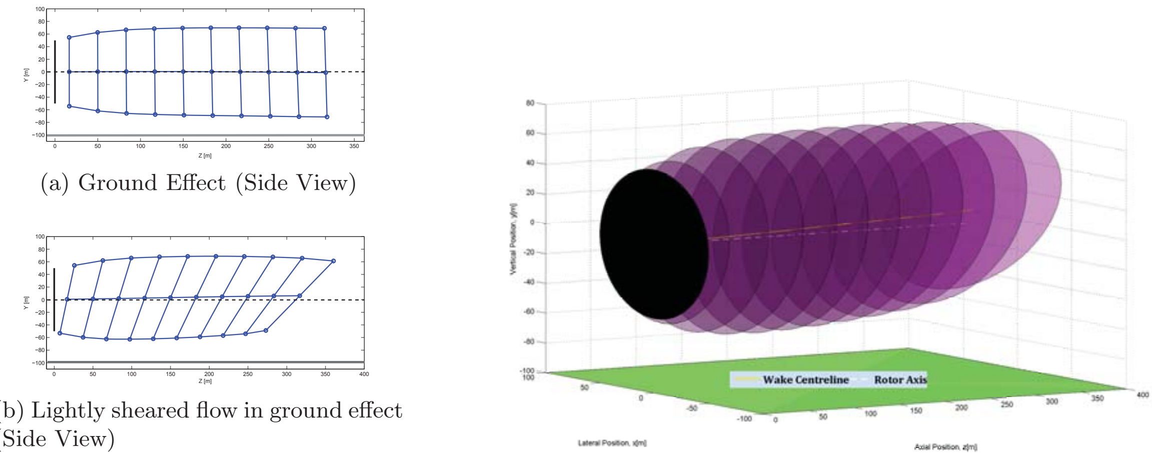

(a) Ground Effect (Side View)

(b) Lightly sheared flow in ground effect (Side View)

(c) Wake Visualisation in sheared flow and ground effect

Figure 3: Rotor wake after 10 revolutions for the case of optimal induction

For offshore wind turbines, the down-shifting tendency could be expected to play a more prominent role in wake aerodynamics since not only are turbulence intensities lower out at sea, but rotors are relatively closer to the ocean surface, compared to their onshore counterparts. The observed down-shifting behaviour would thus seem to imply that for offshore wind turbines, the rotor wakes could be expected to dissipate quicker due to stronger interaction with the ocean surface, resulting in lower overall wind farm losses.

Results also indicate that the stability of the vortex ring system and the overall evolution of the wake are particularly sensitive to the proximity of successive rings, as well as the relative ring strength. An increase in both leads to stronger interaction and the pairing instability is observed, after which the model offers limited insight since it is not able to simulate the actual merging of the rings. The results presented were at most evaluated at the ideal thrust coefficient of $C_T = 8/9$. In general it was observed that close to this value, the simulated dynamic behaviour of the vortex rings became overly chaotic. Model limitations therefore constrain the interpretation of results at high thrust coefficients. These results do however illustrate that at higher operating thrust coefficients, rotor wakes can be expected to display increasingly chaotic and unstable behaviour, especially when subject to shear and yawed inflow, and operation in ground effect.

4.2. Vortex ring interactions

The previous analysis highlighted the importance of the wake pitch and relative strength of the wake elements, for the overall development of the wake. The empirical evidence of vortex pairing events in the wake of ship propellers [10] and helicopter rotors in hover [9] further motivates the current investigation. A comparison is drawn with respect to the evidence given in Medici and Alfredsson [1] of the low periodic frequency signal detected in the wake of a model turbine. The premise is that the pairing instability may be able to explain this observed periodic behaviour. These authors define the Strouhal number St in order to examine characteristic frequencies:

$$St = \frac{fD}{U_\infty} \tag{7}$$

where D is the rotor diameter, U_∞ is the freestream velocity ($0.18m$ and $8.3m/s$, as defined in [1]) and $f(s^{-1})$, the vortex shedding frequency. The same definition is used in the present

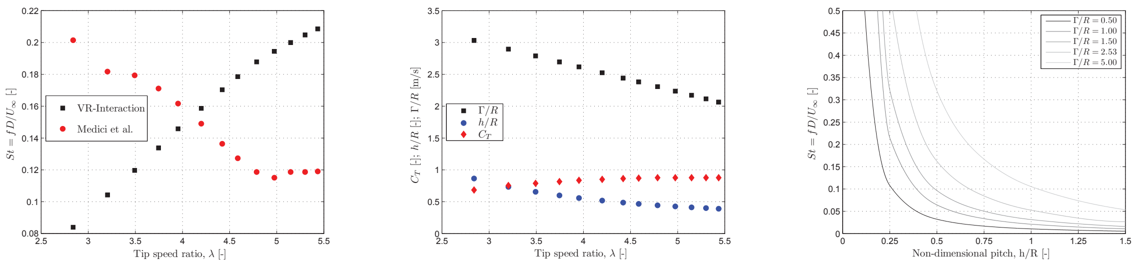

(a) St as a function of tip speed ratio in axial flow, $U_\infty = 8.3m/s$

(b) Pitch, strength and thrust simulation parameters extracted from [1]

(c) Leapfrog frequency as a function of pitch and strength

Figure 4: Vortex ring leapfrogging behaviour and the proposed vortex shedding phenomenon in Medici and Alfredsson [1].

study to facilitate comparisons. Two identical vortex rings (designated *Ring-1* and *Ring-2*) are defined in space, separated by the pitch h. Key model requirements were therefore identified:

(i) the relative ring radii, R_1/R_2
(ii) the relative ring strengths, Γ_1/Γ_2
(iii) the linear pitch of the vortex rings, $h = z_1 - z_2$

Using the results in [1] as a benchmark, it was required to extract the above listed parameters from their experimental data. The following simple relations were defined in order to formulate useful model inputs and are shown in Figure 4b:

(i) the two-bladed model turbine used in this case had a radius of approximately $0.09m$, and this was assigned as the ring radii
(ii) equations 4 and 5 were employed to estimate the strength of each ring, from knowledge of the operational tip speed ratio and the thrust coefficient
(iii) the ring pitch is estimated for a bi-helical wake system using the following approximation:

$$h = U_\infty(1 - a_z) \cdot \frac{\Delta T}{B}, \tag{8}$$

where $\Delta T = \frac{2\pi R}{\lambda U_\infty}$ is the rotational period and a_z is an estimate for the average induced axial velocity based on simple momentum theory and knowledge of C_T.

For the desired dataset, $\lambda_{opt} = 3.66$ and $C_{T(opt)} = 0.794$. Extracting the data points presented in [1] corresponding to the salient tip speed ratio of $\lambda = 4.2$, the simplified analysis using equations 4,5 and 8 yields $\Gamma/R = 2.53m/s$, $h/R = 0.52$ and $R = 0.09m$ as example simulation inputs. The resulting temporal and spatial trajectories are displayed in Figure 5 and the comparison for the full set of data is shown in Figure 4a. Observing the temporal evolution of the rings, it is clearly seen that the period of oscillation of the ring radii is approximately $0.14s$, or $7.14Hz$. In terms of the non-dimensional St number, this corresponds to a value of 0.16, compared with approximately $St = 0.15$ as reported in the benchmark data. Despite the seeming agreement at this operating point, the trend in St with tip speed ratio is different, suggesting that there is no correlation between the dynamics of the pairing instability and the periodicity in the results of Medici et al. [1], as shown in Figure 4a. A higher tip speed ratio and thrust coefficient leads to a finer pitch and weaker vorticity, resulting in an overall stronger interaction and a higher St. In Figure 4c, the leapfrogging frequency of two vortex rings is shown as a function of the strength and pitch for rings of $R = 0.09m$.

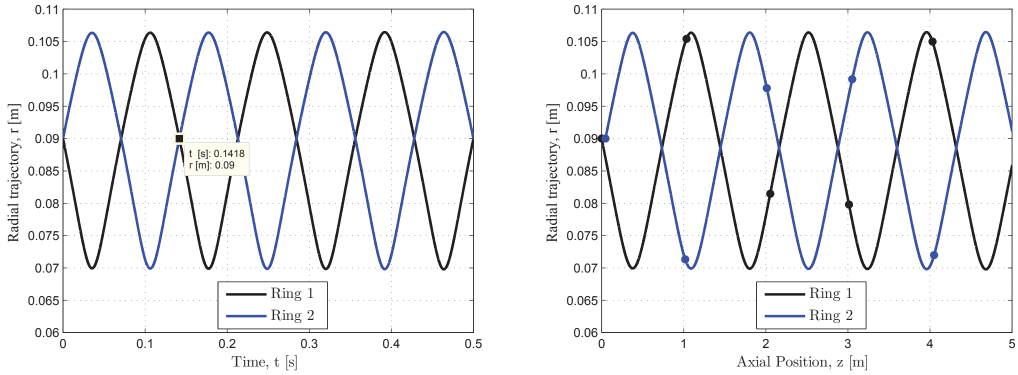

(a) Temporal evolution of VR-system trajectory (b) Spatial evolution of VR-system trajectory; circular markers (●) spaced at $\Delta t = 0.1s$ intervals.

Figure 5: Characteristic leapfrogging frequency obtained using data extracted from Medici and Alfredsson [1]

5. Conclusions

The simple FWVRM described has been shown to correctly predict trends in the wake development of HAWTs. Wake skewing and tilting has been observed at different angles of yaw and in shear flow. For all angles of yaw tested, the wake skew angle was found to be consistently larger than the yaw angle, in accordance with theory and experimental evidence. Upward and downward shifts in the wake structure were observed in shear flow and operation in ground effect respectively. The simplicity of the model has allowed for a useful insight into the effect of the wake self-induction in response to externalities such as shear, yaw and the presence of the ground.

Vortex filament interactions have been addressed mainly in relation to the periodic velocity signals reported in Medici et al. [1]. Although comparable in magnitude, no correlation was found between the vortex shedding frequency proposed in [1] and the interaction frequency of vortex rings. Wake interaction has however been observed experimentally in propeller wakes and this study has illustrated that in normal wind turbine operating conditions, mutual interaction is indeed possible. This points towards the possible role mutual interaction plays in the evolution of the rotor far wake and the need to experimentally investigate this far-wake phenomenon further.

The role of atmospheric turbulence on the meandering of a wind turbine wake may likely be the single most influential factor determining the *transport* of a wind turbine wake. However, through simple means it has been shown that additional external factors can indeed *trigger* destabilising mechanisms within the wake.

Acknowledgments

The research work disclosed in this publication was partially funded by the Strategic Educational Pathways Scholarship (Malta). This scholarship is part-financed by the European Union - European Social Fund (ESF) under Operational Programme II - Cohesion Policy 2007-2013, "Empowering People for More Jobs and a Better Quality of Life".

Appendix A.

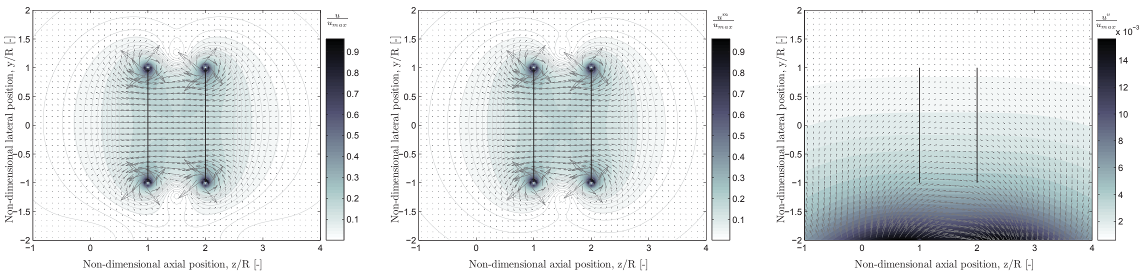

(a) Total velocity (b) Mutual induced velocity (c) Ground-induced velocity

Figure A1: 2D velocity field ($y - z$ plane), induced by a dual-vortex ring system in ground effect; ground position $y/R = -2$.

References

[1] D. Medici and P. H. Alfredsson. Measurements on a wind turbine wake: 3d effects and bluff body vortex shedding. *Wind Energy*, 9(3):219–236, 2006.
[2] G. España, S. Aubrun, S. Loyer, and P. Devinant. Spatial study of the wake meandering using modelled wind turbines in a wind tunnel. *Wind Energy*, 14(7):923–937, 2011.
[3] F. Bingöl, G. C. Larsen, and J. Mann. Wake meandering - an analysis of instantaneous 2d laser measurements. *Proc. Torque 2010: The science of making torque from wind*, 75, 2007.
[4] G. C. Larsen et al. Dynamic wake meandering modelling. Technical Report Risø-R-1607(EN), Risø National Laboratory: Roskilde, 2007.
[5] G. Hassan. Dynamic loads in wind farms ii. Technical Report JOU2-CT92-0094, 1996.
[6] J. Sørensen and V. Okulov. Modelling of the far wake behind a wind turbine. In J. Peinke, P. Schaumann, and S. Barth, editors, *Proc. of Euromech Colloquium on Wind Energy*, 2007.
[7] S. E. Widnall. The stability of a helical vortex filament. *J. Fluid Mech.*, 54:641–663, 1972.
[8] J. Sørensen and V. Okulov. Stability of helical tip vortices in a rotor far wake. *J. Fluid Mech.*, 576:1–25, 2007.
[9] J. Stack, F. X. Caradonna, and S. Ömer. Flow visualizations and extended thrust time histories of rotor vortex wakes in descent. In *AHS 4th Decennial Specialists' Conf. on Aeromechanics*, 2004.
[10] M. Felli, R. Camussi, and F. di Felice. Mechanisms of evolution of the propeller wake in the transition and far field. *J. Fluid Mech.*, 682:5–53, 2011.
[11] S. Øye. A simple vortex model of a wind turbine rotor. *Proc. 3rd IEA Symp. on the Aerodynamics of Wind Turbines, ETSU*, Harwell, Didcot, UK, 1989.
[12] D. Micallef, C. J. Simão Ferreira, T. Sant, and G. J. W. van Bussel. An analytical model of wake deflection due to shear flow. *Proc. Torque 2010: The science of making torque from wind*, 2010.
[13] R. E. Wilson. Wind turbine flow field model. *J. ASME*, 108:344–345, 1986.
[14] M. Abramowitz and I. Stegun. *Handbook of Mathematical Functions.* Dover Publications, 1965.
[15] S. S. Yoon and S. D. Heister. Analytical formulas for the velocity field infuced by an infinitely thin vortex ring. *Int. J. of Numerical Methods in Fluids*, 44:665–672, 2004.
[16] H. Lamb. *Hydrodynamics.* Dover Publications, 1934.
[17] V. V. Meleshko. Coaxial axisymmetric vortex rings: 150 years after helmholtz. *Theoretical and Computational Fluid Dynamics*, 24:403–431, 2010.
[18] F. Grasso. Awsm ground and wind shear effects in aerodynamic calculations. Technical Report ECN-E-10-016, Energy Research Centre Netherlands, 2010.
[19] A. M. Talmon. The wake of a hawt, measurements in uniform approach flow and in a simulated boundary layer. Technical Report 85-01021, TNO Division of Technology for Society, 1985.
[20] A. M. Talmon. A wind tunnel investigation into the effects of tower and nacelle on wind turbine wake flow. Technical Report 84-08479, TNO Division of Technology for Society, 1984.
[21] A. Crespo, J. Hernández, E. Fraga, and C. Andreu. Experimental validation of the upm computer code to calculate wind turbine wakes and comparison with other models. *J. Wind Eng. Ind. Aerodynamics*, 27:77–88, 1988.